ISSN 1870-4069

Diabetic Retinopathy Detectio Via Local Binary Patterns

David Ferreiro-Piñeiro, Ivan Olmos Pineda,
Arturo Olvera López

Benemérita Universidad Autónoma de Puebla,
Mexico

david.ferreiro@alumno, {ivan.olmos,
jose.olvera}@correo.buap.mx

Abstract. Diabetic Retinopathy (DR) is the leading cause of preventable blindness for working-age people. Clinical detection methods are expensive, time-consuming, and subjective. Therefore, automated techniques have been proposed to develop complementary objective tools to support the diagnosis that facilitate its detection. In this work, we offer an approach for detecting DR in retinal images using a texture descriptor. The behavior of two different implementations of the Local Binary Patterns (LBP) is analyzed in the APTOS database, using sliding windows mechanisms to extract a more significant amount of detail from the descriptors used. The classification is carried out via a Support Vector Machines (SVM) whose training and evaluation are performed using cross-validation. The experimental results of the two implementations are compared; the model based on uniform LBP obtained the best performance with an accuracy of 0.935, a sensibility of 0.924, and a specificity of 0.947, demonstrating that the extraction of relevant features using uniform LBP guarantees the detection of DR.

Keywords: Diabetics retinopathy, LBP, uniform LBP.

1 Introduction

The lifestyle habits in populations determine the evolution of new diseases such as Diabetes. This kind of disease causes an increment in sugar levels in the blood, affecting retinal tissue and evolving into a condition known as Diabetic Retinopathy (DR). According to the World Health Organization (WHO), 146 million people suffer from DR, which is the leading cause of blindness for productive people [1, 2].

DR is a progressive and degenerative disease that causes pathological changes in retinal tissue, and its diagnosis depends on the detection of lesions through observation and analysis from ophthalmologists. According to the lesions found, ophthalmology classifies the disease in five stages: healthy, mild, moderate, severe, and proliferative (PDR) (Fig. 1 shows the evolution of these kinds of lesions).

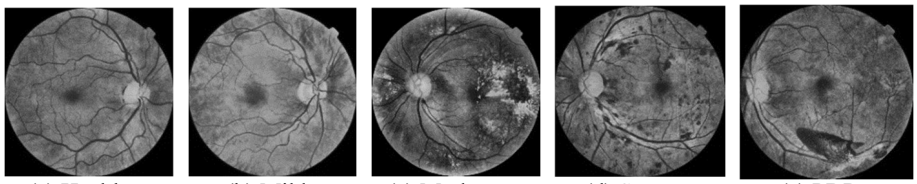

(a) Healthy (b) Mild (c) Moderate (d) Severe (e) PDR

Fig. 1. Clinic evolution to the Diabetic Retinopathy (Source: Decencière et al. [5]).

The clinical manifestations of the disease are microaneurysms, hemorrhages, exudates [3], and new defective blood vessel or vascular abnormalities, which can lead to retinal detachment and vision loss.

The clinic method for diagnosis is expensive and requires qualified specialists; the diagnosis quality sometimes depends on subjective factors such as exhaustion, stress, and experience. For these reasons, the WHO recommends strengthening research to expand technological advances to help people with this type of condition [4].

Timely detection of DR has become a field of research for the development of computer vision and artificial intelligence applications. The main approaches are oriented to the detection of specific lesions to conduct classification tasks or to the development of models based on deep learning.

The proper diagnosis depends not only on the detection of the lesions but also on their location in the retinal tissue. In the present investigation, a diagnostic model for DR is proposed using classic computer vision techniques that allow the detection and identification of specific lesions to be dispensed with and guarantee the diagnosis of the disease; considering the limited availability of retinal images, it does not suggest using deep learning approaches.

Diagnosis determines the presence of the disease in retinal images. The proposed models are helpful as a complementary diagnostic mechanism for modern technologies that allow the attention of ophthalmological care while reducing cost and guaranteeing access to the most vulnerable population.

This work is organized as follows: Section 2 developed a study of state of art related to the use of SVM in the detection of DR. Section 3 presents a methodological proposal from the pre-processing of the images, the study of the different implementations of the LBP, the experimental development, and the discussion of the results. Finally, the conclusions of the work are presented.

2 Related Works

The analysis of the literature allowed us to identify five main working approaches during the automatic diagnosis of DR: based on regions (oriented to the detection of specific lesions designing the relevant characteristics), modification of known Convolutional Neural Network (CNN) models, hybrids (use CNN to extract relevant features, for the classification they use other traditional classifiers), development of new architectures and hyperparameter tuning (improve system performance by modifying specific parameters).

The work proposed by AbdelMaksoud et al. [6] is oriented to the detection and analysis of the pathological changes that affect the retina during the development of DR, performing the segmentation of specific lesions (microaneurysms, exudates, and hemorrhages). Characteristics are extracted using different techniques such as the Gray Level Co-Occurrence Matrix, the area of the blood vessels, the bifurcation points, and determined the number of lesions in the images.

After the characteristics are extracted, a classification model is developed based on multilabel SVM on the public databases DRIVE, Messidor, Stare, and IDRiD, reporting an accuracy of 0.892. Issac et al. [7] perform a quantitative analysis of the red, bright lesions and the optic disc present in the images. From these data extracted, ten characteristics and the classification using the Messidor-1 and DIARETDB0 databases.

The authors highlight lesions by intensity normalization and thresholding for detection to improve experimental results. They obtained an accuracy of 0.9213, a sensitivity of 0.9285, and a specificity of 0.8 in the DIARETDB0 database. Another approach (Katada et al.) [8] proposes a hybrid architecture of Inception-V3 and SVM on a private database of two hundred images corresponding to patients of Japanese ethnicity and on the EyePACS database.

The main contribution is that the models can be abstracted from ethnic traits, representing an advantage due to the limited availability of data from non-Anglo-Saxon patients. A sensitivity of 0.815 and 0.908, and specificity of 0.719 and 0.9, are reported for EyePACS and the private database, respectively. Another approach estimates the probability of disease development from the location of microaneurysms and hemorrhages on retinal images [9].

The idea developed by the authors not only segment the lesions but also find them and determine their relevance. The authors employ transfer learning techniques to mitigate limited data availability. Son et al. [10] develop independent models to detect twelve different lesions: hemorrhages, hard exudates, soft exudates, retinal scars, any vascular abnormality, and nerve fiber layer defects, among others; these algorithms are based on the information provided by the region.

The proposed architecture allows detecting multiple lesions, combining various models, and visualizing them with a heat map as an auxiliary output to identify the aspects considered by the algorithm to generate the final classification. There is a tendency to use approaches based on deep learning; these approaches require a considerable volume of data to perform their training and validation.

In addition, recent works are oriented to supply an adequate solution to the problem and explain how that solution is reached. This allows the introduction of external specialists to validate the proper functioning of the systems.

3 Methodological Proposal

The methodological proposal is shown in Fig. 2. The first step is a pre-processing phase; then, relevant features are extracted to perform the classification process. This article is oriented to the analysis of the texture in the different regions of the image to conduct the diagnosis of DR without it being necessary to detect the specific lesions present in the tissue. The proposal classifies the input image as healthy or sick, although it can be

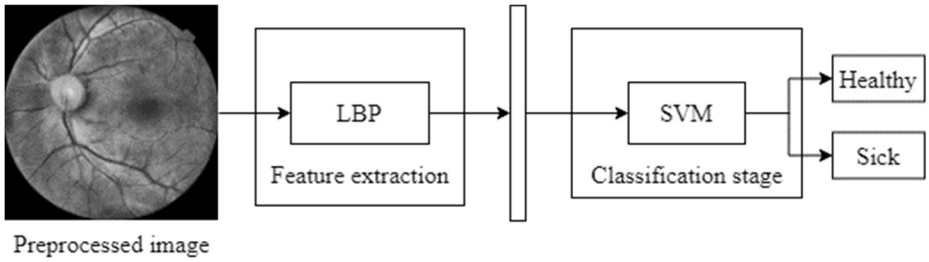

Fig. 2. Proposed methodological scheme.

extended to the detection of PDR, which considers the degree of evolution of the disease.

3.1 Pre-Processing Steps

The models were developed and evaluated on images from a public tagged repository managed within the framework of the 4th Symposium of the Asia Pacific Tele-Ophthalmology Society (APTOS). These images were captured under different lighting conditions, techniques and instruments and included the retinal tissue, its vascular network, macula, and optic disc. This region is surrounded by an area that does not provide helpful information, making processing work difficult.

The pre-processing, the retinal tissue is delimited by segmenting the brightness channel by applying the Otsu method in the HSV color space, determining the transition points between the tissue and the surrounding area that define the proper working area. Subsequently, a Gaussian filter is applied with $\sigma = 1$, which reduces the Gaussian noise; a change is made in the color space using the LAB model, which allows the separation of the lighting treatment on the chroma channels.

Contrast-Limited Adaptative Histogram Equalization (CLAHE) is applied on the L channel, modifying the image's lighting without affecting the color components, avoiding the introduction of artifacts that can be confused with lesions. Finally, the dimensions of the pictures are homogenized to 600 × 600 pixels.

3.2 Feature Extraction

Feature extraction is a crucial stage for the development of a classification model. It allows for defining the distinctive features for detecting the disease and describing its clinical grade. This work proposes to develop this process considering the textures of retinal images. The textures are repetitive patterns in local intensity differences that allow differentiated structures [11].

Different texture descriptors include Gray Level Co-Occurrence Matrix (GLCM), Binary Local Patterns (LBP), and Gabor filters, among others. This descriptor aims to quantify the qualities that we intuitively define as rough, silky, or soft and that we commonly use depending on the intensity variation of the pixels.

The main differences between these descriptors are how they process spatial information. GLCM generates second-order statistics from the definition of co-occurrence matrices, according to the distances and the direction of analysis.

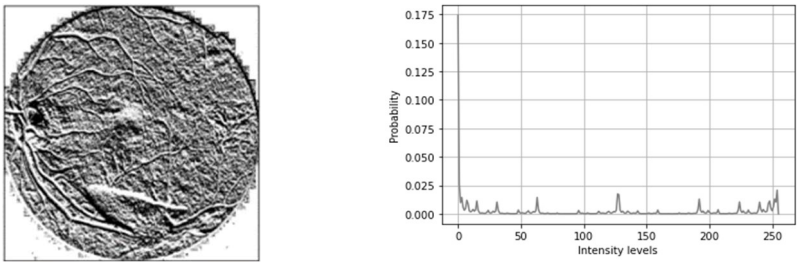

(a) LBP image (b) LBP image histogram

Fig. 3. Analysis of the behavior of the classic LBP extractor.

This descriptor suffers from high dimensionality, consumes large amounts of memory, and its derived features have a high correlation [12].

Gabor filters emulate the human vision process but require adjustments regarding the orientation of the filters. Orientation is a critical aspect because the detection of the characteristics in the images depends on their excellent tuning. Filter banks are used to solve this problem by processing the images in different orientations, and this increases the computational requirements.

The LBP approach is considered to extract texture features using a circular neighborhood where the texture is defined as the joint distribution of the gray levels described as the equidistance between the central pixel and the radius of the neighborhood. From the fundamental characteristics of the previously exposed descriptors, it was decided to use the LBP during the experimental development of the present investigation. According to [13], the LBP descriptor can be expressed as:

$$\text{LBP} = \sum_{p=0}^{P-1} s(g_p - g_c)2^p, \tag{1}$$

$$s(g_p - g_c) = \begin{cases} 1 & \text{if } g_p - g_c \geq 0, \\ 0 & \text{if } g_p - g_c < 0, \end{cases} \tag{2}$$

where g_c is the central pixel intensity, g_p is the intensity of the neighboring pixel and finally 2^p quantization weights. When applying this descriptor, the exudates are represented as craters on the retina's surface; the hemorrhages or microaneurysms are described as plains or elevations in the retinal tissue; these results can be visualized in Fig. 3a, the relief generated by the hemorrhage is observed, allowing its identification.

LBP allows obtaining the histograms that describe the image and is invariant to rotation. The property of invariance to rotation is crucial, the retinal images can be taken from different angles, and descriptors must characterize the presence of the disease regardless of the spatial distribution of the characteristic lesions in the retina.

Then, this descriptor allows us to differentiate between the types of the characteristic lesion and, therefore, could be used as a discriminator. Fig. 3-b shows the input image's histogram; it can be noticed how the image is distributed over the entire dynamic range.

Histogram-based approaches can be ambiguous in describing large regions; sliding window mechanisms are used to avoid this problem. The descriptor for specific areas

Table 1. Comparison considering some state-of-the-art methods.

Model	Auc	Acc	Se	Sp
Uniform LBP	0.97	0.935	0.924	0.947
Classical LBP	0.97	0.927	0.924	0.93
AbdelMaksoud et al. [6]	0.89		0.85	0.85
Issac et al. [7]		0.92	0.92	0.8
Katada et al. [8]			0.90	0.80

is determined and concatenated to form a single feature vector. This approach strengthens feature detection and, when using LBP, helps guarantee the descriptor's translation invariance. To use this approach, the proper selection of the size of the windows is essential; large windows lose the details, and small windows cannot determine the presence of specific lesions.

The output feature vector would be equal to $\vec{V} = 256 \times N$, where N is the number of sliding windows and 256 are the intensity levels of the histograms using the proposed approach. This approach consumes expensive computing resources.

One way to reduce computational requirements is to consider the presence of uniform patterns during LBP encoding. When the pixels surrounding the central pixel do not alternate or contain at most two transitions, this pattern is considered uniform, otherwise called non-uniform [14]. This descriptor can be expressed as:

$$\mathrm{LBP}_{P,R}^{\mathrm{riu2}} = \begin{cases} \sum_{P=0}^{P-1} s(g_p - g_c) & \text{if } U(LBP_{P,R} \leq 2), \\ P+1 & \text{other case,} \end{cases} \tag{3}$$

$$U(LBP_{P,R}) = |s(g_{P-1} - g_c)| + \sum_{P=1}^{P-1} |s(g_P - g_c) - s(g_{P-1} - g_c)|, \tag{4}$$

where P number of pixels in the circular neighborhood determines the angular resolution, R radius of the circular neighborhood determines the spatial resolution, and finally $LBP_{P,R}$ is a measure of uniformity. It has shown that combinations of uniform patterns and the rotation invariance property can be encoded with $P + 1$ levels of intensity, and all non-uniform patterns are represented with an additional intensity level.

It might be thought that a significant loss of information may occur by using uniform LBP. However, based on the uniform LBP results (**¡Error! No se encuentra el origen de la referencia.**-a), it can be noticed that the details that define the presence and location of a lesion are still preserved. According to these results, it is possible to represent relevant information considering a lower amount of intensity level.

In **¡Error! No se encuentra el origen de la referencia.**-b, the histogram generated using the uniform approach $\mathrm{LBP}_{36,3}^{\mathrm{riu2}}$ is depicted. In this case, the output vector is modified and will have a length of $\vec{V} = 38 \times N$ due to the properties of the analyzed images, the descriptor considers an angular resolution of 10°.

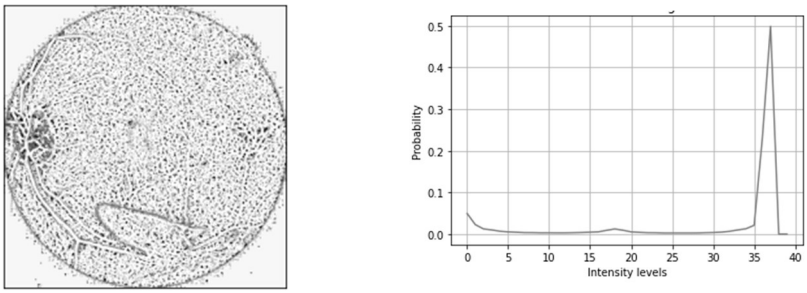

(a) Uniform LBP image. (b) Uniform LBP image histogram.

Fig. 4. Uniform LBP image analysis.

3.3 Classification Stage

Feature extraction was performed considering the use of sliding window techniques. The size of the windows was defined in 100 x 100 pixels, with a 50% overlap between adjacent windows to increase the redundancy of the extracted features.

A total of 144 windows or analysis segments were generated in which the LBP vector is determined. The uniform LBP vector will have a dimension of 5472 elements as opposed to the 36720 elements of the classical LBP vector.

The APTOS database contains a population of 5593 images, of which 3662 are labeled [15]. These images were classified according to the degree of clinical evolution of the disease (healthy, mild, moderate, severe, proliferative). For the present work, they were grouped in a binary way into healthy or sick, and stratified random sampling to preserve the ratio classes in the original training set is conducted. The training and test sets were formed considering 80% and 20%, respectively.

In addition, the selection of the hyperparameters of the models was conducted using a genetic optimization algorithm. This algorithm was applied to the models developed in the classical LBP and uniform LBP features. An SVM with a degree three polynomial kernel was designed to address the uniform LBP features, and an SVM with a radial basis function kernel for de classical LBP features.

The model was validated, applied a ten cross-validation, and analyzed the area under the ROC curve as a metric of interest, which is a standard metric for comparing the experimental results of applications oriented to medical services [16]. In Fig. 5, the confusion matrices generated when evaluating the classification models on the test images are depicted.

The metric used to evaluate the performance of the developed models are the area under the ROC curve (Auc), accuracy (Acc), sensitivity (Se), and specificity (Sp). A priori analysis allows us to establish that the model based on uniform LBP has a better behavior than the classic LBP model. However, in medical environments, it is more significant to achieve high sensitivity, reducing the occurrence of false negatives. False positives can be corrected by performing complementary clinical tests, unlike false negatives that could stop the treatment of the disease.

The uniform LBP model has a higher sensitivity by reporting fewer false negatives, around 3.8% versus 2.7% false positives. While the model developed on classic LBP

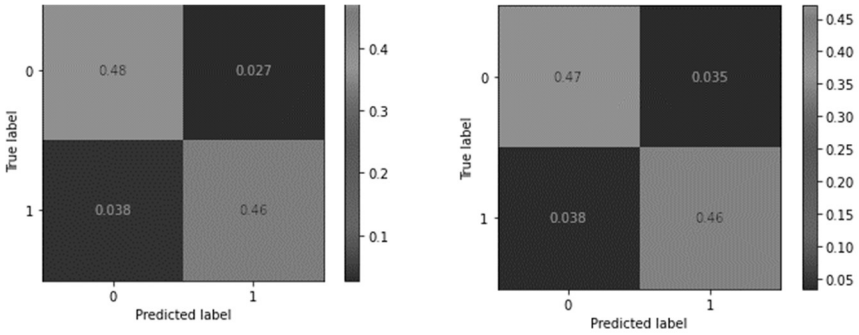

(a) Uniform LBP (b) Classical LBP

Fig. 5. Experimental confusion matrices.

has the opposite behavior, it has a higher number of false negatives (3.8%) than the false positives detected. Therefore, both models have the same sensitivity, but the uniform LBP has better specificity and accuracy. In Table 1, the main experimental results obtained are observed in comparison with other models reported in state-of-the-art. Based on our preliminary results, the proposed methodology allows the detection of characteristic lesions simply in the form of reliefs in the retinal tissue.

It, therefore, allows detecting the presence of the DR. The uniform LBP descriptor guarantees to extract the relevant features to conduct the detection using a vector of a small length without losing relevant information, which is particularly useful in limited computational resources environments.

4 Conclusions

Two classification models were developed and evaluated using support vector machines and texture descriptors to detect Diabetic Retinopathy in retinal pictures. The descriptors used guaranteed the exact spatial and angular resolution but differed in their form to encode the results. The implementations differed in the number of elements considered in the feature vectors.

The model developed on the uniform LBP obtained a similar performance in the ability to detect the presence of the disease (sensitivity) and in the area under the ROC curve and superior performance in the specificity and accuracy of the classification when compared with the model developed on the classic LBP.

From this, it was found that the number of features used does not determine, in general, the quality of the classification models. The model based on the classic LBP is sensitive to the presence of artifacts or other variations in the images, aspects to which the uniform implementation is invariant.

In addition, the proposed model of better results was compared with some works reported in state of the art, with encouraging results, although it would be interesting to evaluate this model on the same databases used by other authors. In future work, it is necessary to evaluate the behavior of the model developed on other public databases to validate the results and be able to make an objective comparison of the results.

References

1. World Health Organization: World report on vision. World Health Organization (2019) www.who.int/publications/i/item/9789241516570
2. Kumar, S., Adarsh, A., Kumar, B., Singh, A. K.: An automated early diabetic retinopathy detection through improved blood vessel and optic disc segmentation. Optics and Laser Technology, vol. 121, pp. 105815 (2020) doi: 10.1016/j.optlastec.2019.105815
3. Saranya, P., Prabakaran, S.: Automatic detection of non-proliferative diabetic retinopathy in retinal fundus images using convolution neural network. Journal of Ambient Intelligence and Humanized Computing, Springer Science and Business Media (2020) doi: 10.1007/s12652-020-02518-6
4. World health organization: Recommendations on digital interventions for health system strengthening. WHO Guideline (2019) www.who.int/publications/i/item/9789241550505
5. Decencière, E., Zhang, X., Cazuguel, G., Lay, B., Cochener, B., Trone, C., Gain, P., Ordonez, R., Massin, P., Erginay, A., Charton, B., Klein, J. C.: Feedback on a publicly distributed image database: the messidor database. Image Analysis and Stereology, Slovenian Society for Stereology and Quantitative Image Analysis, vol. 33, no. 3, pp. 231 (2014) doi: 10.5566/ias.1155
6. AbdelMaksoud, E., Barakat, S., Elmogy, M.: A comprehensive diagnosis system for early signs and different diabetic retinopathy grades using fundus retinal images based on pathological changes detection. Computers in Biology and Medicine, vol. 126, pp. 104039 (2020) doi: 10.1016/j.compbiomed.2020.104039
7. Issac, A., Dutta, M. K., Travieso, C. M.: Automatic computer vision-based detection and quantitative analysis of indicative parameters for grading of diabetic retinopathy. Neural Computing and Applications, vol. 32, no. 20, pp. 15687–15697 (2018) doi: 10.1007/s00521-018-3443-z
8. Katada, Y., Ozawa, N., Masayoshi, K., Ofuji, Y., Tsubota, K., Kurihara, T.: Automatic screening for diabetic retinopathy in interracial fundus images using artificial intelligence. Intelligence-Based Medicine, vol. 3–4, pp. 100024 (2020) doi: 10.1016/j.ibmed.2020.100024
9. Zago, G. T., Andreão, R. V., Dorizzi, B., Teatini Salles, E.: Diabetic retinopathy detection using red lesion localization and convolutional neural networks. Computers in Biology and Medicine, vol. 116, pp. 103537 (2020) doi: 10.1016/j.compbiomed.2019.103537
10. Son, J., Shin, J. Y., Kim, H. D., Jung, K. H., Park, K. H., Park, S. J.: Development and validation of deep learning models for screening multiple abnormal findings in retinal fundus images. Ophthalmology, vol. 127, no. 1, pp. 85–94 (2020) doi: 10.1016/j.ophtha.2019.05.029
11. Chaki, J., Dey, N.: Texture feature extraction techniques for image recognition. Springer Singapore (2020) doi: 10.1007/978-981-15-0853-0
12. Hall-Beyer, M.: Practical guidelines for choosing GLCM textures to use in landscape classification tasks over a range of moderate spatial scales. International Journal of Remote Sensing, Informa UK Limited, vol. 38, no. 5, pp. 1312–1338 (2017) doi: 10.1080/01431161.2016.1278314
13. Ojala, T., Pietikainen, M., Maenpaa, T.: Multiresolution gray-scale and rotation invariant texture classification with local binary patterns. IEEE Transactions on Pattern Analysis and Machine Intelligence, vol. 24, no. 7, pp. 971–987 (2002) doi: 10.1109/tpami.2002.1017623
14. Ahonen, T., Hadid, A., Pietikainen, M.: Face description with local binary patterns: application to face recognition. In: IEEE Transactions on Pattern Analysis and Machine Intelligence, vol. 28, no. 12, pp. 2037–2041 (2006) doi: 10.1109/tpami.2006.244
15. Kagle: APTOS 2019 Blindness Detection (2022) www.kaggle.com/competitions/aptos2019-blindness-detection/overview

16. Hanley, J. A., McNeil, B. J.: The meaning and use of the area under a receiver operating characteristic (ROC) curve. Radiology, Radiological Society of North America, vol. 143, no. 1, pp. 29–36 (1982) doi: 10.1148/radiology.143.1.7063747